Fold growth rates in 3D buckle folds

Marcel Frehner

Geological Institute, ETH Zurich, Switzerland, marcel.frehner@erdw.ethz.ch

Summary

Geological folds are inherently 3D structures; therefore they also grow in three dimensions. Here, fold growth in all three dimensions is quantified by numerically simulating upright single-layer folds in 3D Newtonian media. Horizontal uniaxial shortening leads to a buckling instability, which grows from a point-like initial perturbation in all three dimensions by fold amplification (vertical), fold elongation (parallel to fold axis), and sequential fold growth (parallel to shortening direction) The two lateral directions exhibit similar averaged growth rates leading to bulk fold structures with aspect ratios close to 1. However, fold elongation is continuous with increasing bulk shortening, while sequential fold growth exhibits jumps whenever a new sequential fold appears. Compared to the two lateral growth directions, fold amplification exhibits a slightly higher growth rate.

1. Introduction

Geological folds are important natural features for structural geologists. In the field, the orientation and geometry of small-scale folds in the three-dimensional (3D) space helps identify larger-scale structures not visible in one single outcrop. Fold structures also provide an essential basis for tectonic interpretations, for example for estimating tectonic shortening directions. Equally important, the wavelength, the arclength, and the overall geometry of a fold are functions of the rheological parameters of a folded rock layer and its surrounding matrix. Therefore, analyzing the shape of a fold can reveal information about the rheological properties of the involved rocks (Huddleston and Treagus, 2010).

The fold shape that can be observed in the field is a result of the fold growth history. Therefore, it is essential to not only describe the fold shape but also to understand the process of fold growth. Geological folds are inherently 3D structures; hence their growth also needs to be studied in 3D.

Definitions of 3D fold growth

To avoid confusion, the following terminology for fold growth in 3D is used here, using the coordinate system defined in Figure 1:

- Fold amplification (growth in z-direction) describes the growth from a fold shape with low limb-dip angle to a shape with larger limb-dip angle.
- Fold elongation (growth in y-direction) is parallel to the fold axis and describes the growth from a dome-shaped (3D) structure to a more cylindrical fold (2D).
- Sequential fold growth (growth in x-direction) is parallel to the shortening direction and describes the growth of additional folds adjacent to the initial isolated fold. The initial fold is termed 0th sequential fold; later grown folds are numbered consecutively.

Here, *lateral fold growth* is used as an umbrella term for both fold elongation and sequential fold growth.

Aim of this study

Existing studies do not quantify all three growth directions at once. Analytical solutions for 3D folding (e.g., Fletcher, 1991) neglect the two lateral growth rates because a periodic initial perturbation is assumed. The few numerical 3D folding studies (e.g., Schmid et al., 2008) do not quantify fold growth, but rather investigate one specific 3D phenomenon (e.g., linkage). The aim of the presented study is to numerically simulate simplified test cases of 3D folding and to quantify fold growth in all three dimensions to better understand the first-order relationships between the different growth directions.

2. Model and Methods

3D buckle folding is assumed to be a slow flow process governed by Newtonian rheology. The self-developed finite-element (FE) code solving the corresponding continuum mechanics equations is a 3D version of the code tested and used in Frehner and Schmalholz (2006) and Frehner (2011). The model (Figure 1) consists of a higher-viscosity layer (thickness H_L=1) on top of a lower-viscosity layer (thickness $H_M \gg H_L$) with viscosity ratio R. The model has

a free surface and is compressed horizontally in x-direction with a constant shortening strain rate, $D_{xx}<0$. This corresponds, for example, to pure-shear analog models with lubricated base and side walls or to fold belts, where flow parallel to the fold axes is prohibited.

To allow a mechanical folding instability to develop, a point-like initial perturbation is added to the bottom and top interfaces of the upper layer corresponding to a two-dimensional Gaussian (equation given in Figure 1; A_0=0.01). The effective initial wavelength of the Gaussian is defined as

$$\lambda_0^{\text{eff}} = 2 \times \text{FWHM} = 2 \times \sqrt{8\ln(2)}\sigma \qquad (1)$$

The full width at half maximum (FWHM) corresponds to the circle diameter in the x-y-plane, within which the initial perturbation is larger than $A_0/2$ (i.e., half maximum).
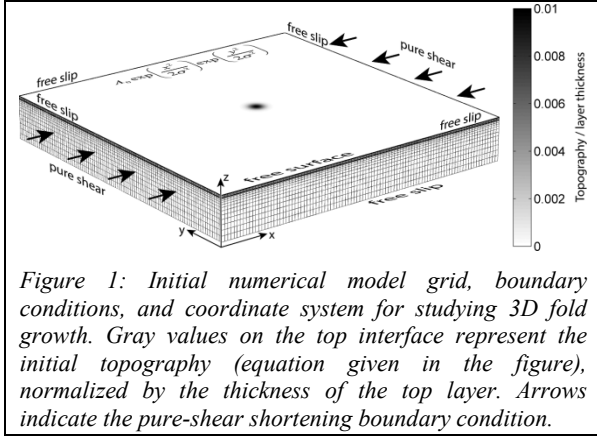

Figure 1: Initial numerical model grid, boundary conditions, and coordinate system for studying 3D fold growth. Gray values on the top interface represent the initial topography (equation given in the figure), normalized by the thickness of the top layer. Arrows indicate the pure-shear shortening boundary condition.

During the FE-simulations, the bulk amplitudes (or extent) of the fold structure in all three coordinate directions are calculated based on the folded upper surface of the model:

- Amplitude in z-direction:

$$A_z = z\big|_{x=0,y=0} - z_{\text{ref}} \qquad (2)$$

- Amplitude in y-direction:

$$A_y = \max(y) \text{ where } z\big|_{x=0} - z_{\text{ref}} = \frac{A_0}{2} \qquad (3)$$

- Amplitude in x-direction:

$$A_x = \max(x) \text{ where } z\big|_{y=0} - z_{\text{ref}} = \frac{A_0}{2} \qquad (4)$$

The reference topography, z_{ref}, is the average of the upper model surface. In Figure 2, A_z corresponds to the color in the model center and A_y and A_x correspond to half the extent of the central contour line in y-direction and to half the maximal extent of all contour lines in x-direction, respectively.

Exponential growth is assumed in all three directions. Taking into account the shortening and extension directions, the exponential bulk amplitude evolution laws are (t is time):

- Exponential growth in z-direction:

$$A_z = A_z\big|_{t=0} \exp\left[-(q_z+1)D_{xx}t\right] \qquad (5)$$

- Exponential growth in y-direction:

$$A_y = A_y\big|_{t=0} \exp\left[-q_y D_{xx}t\right] \qquad (6)$$

- Exponential growth in x-direction:

$$A_x = A_x\big|_{t=0} \exp\left[-(q_x-1)D_{xx}t\right] \qquad (7)$$

Equations (2)–(7) are valid for the fold structure as a whole (bulk values). Similarly, amplitudes can be calculated for each individual sequential syn- and antiform. The amplitudes in z- and y-direction of the initial (or 0th sequential) fold are equal to the bulk amplitudes.

3. Results and Interpretations

As an example, the simulation with viscosity ratio R=100 and initial perturbation σ=6 (Figure 1) is shown and discussed below.

Fold shape evolution and individual folds
Figure 2 shows snapshots of the evolving fold structure with increasing background shortening ($s=1-\exp(D_{xx}t)$). The fold grows in all three dimensions. Fold amplification (z-direction) is evident from the increasing topography (indicated by colors); fold elongation (y-direction) is evident from the elongation of the $A_0/2$ topographic contour line in the model center; sequential fold growth (x-direction) is evident from the sequential appearance of new $A_0/2$ topographic contour lines.

The initial isolated fold starts with normalized amplitudes, aspect ratio, and amplitude ratios all equal to 1 (Figure 3), which represents the initial condition of the simulation. Both the z- and y-amplitudes of the individual folds increase with increasing shortening. At the same time, growth in x-direction of the individual folds is limited to an x-amplitude of around 1 (Figure 3a) showing that the fold structure as a whole grows in x-direction by sequential folding, and not by the growth of one individual anti- or synform. The combination of the two lateral growths leads to an increasing aspect ratio of the initial isolated fold (Figure 3b). New sequential folds appear already with an elevated aspect ratio and continue elongating with further shortening (see also Figure 2). Generally, fold amplitude ratios with the z-

amplitude as the denominator (Figure 3c) decrease with increasing shortening, indicating that fold growth in z-direction exhibits a higher rate than the two lateral directions.
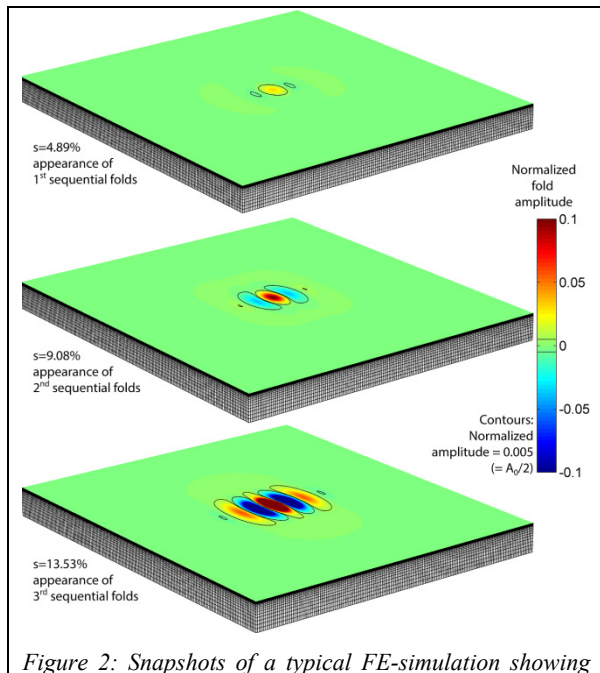

Figure 2: Snapshots of a typical FE-simulation showing the evolution of the 3D fold structure with increasing background shortening, s. The fold amplitude (z-direction) is normalized by the thickness of the top layer; black lines are contour lines of the normalized fold amplitude equal to half the initial value (0.005). The maximum extent in x- and y-direction of these contour lines is used to calculate the fold amplitude in x- and y-direction (Equations (5) and (4)). Parameters for this simulation are: R=100 and σ=6.

Bulk fold amplitudes and growth rates in 3D

Figure 3 also shows the data for the bulk fold structure (thick lines). The bulk amplitudes in z- and y-direction are equal to the amplitudes of the initial isolated fold and increases continuously with increasing shortening. Growth of the fold structure in x-direction (Figure 3a) is marked by sudden jumps every time a new sequential fold appears. Despite these jumps, the average amplitude in x-direction is of the same order as in y-direction leading to an almost constant bulk fold aspect ratio of around 1 (Figure 3b). Such equal growth in both lateral directions also occurs when using different parameter combinations and seems to be a universal feature of 3D fold growth. However, these two lateral growths exhibit a lower rate compared to fold amplification (growth in z-direction) leading to fold amplitude ratios clearly below 1 (Figure 3c). This is also the case for the other tested parameter combinations.

Applying Equations (5)–(7) to the amplitude data in Figure 3a, the fold growth rates in all three directions can be calculated (Figure 4). The fold amplification rate (z-direction) increases slightly (from ~19–25) with increasing shortening (Figure 4a), while the fold elongation rate (y-direction) stays roughly constant at a value of around 10. The sequential fold growth rate (x-direction) exhibits sharp jumps when new sequential folds appear. In the long term, both lateral fold growth rates are similar, represented by a lateral growth rate ratio close to 1 (Figure 4b), and about half of the fold amplification rate (growth rate ratio around 0.5; Figure 4b). This general relationship between the different fold growth rates also occurs for all other tested parameter combinations.
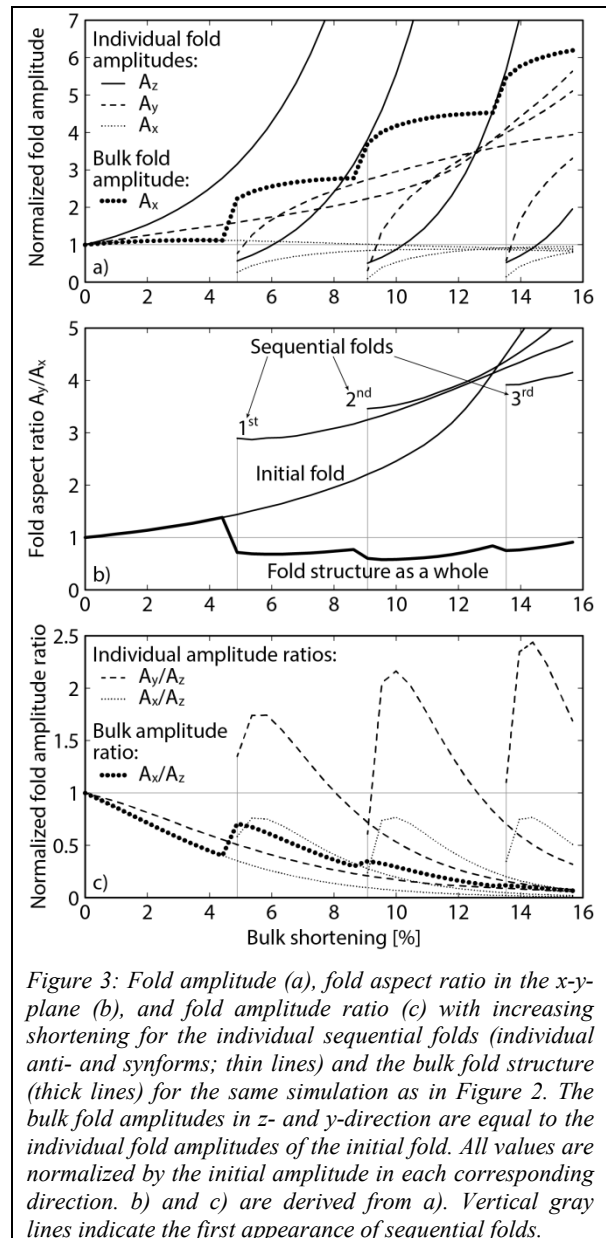

Figure 3: Fold amplitude (a), fold aspect ratio in the x-y-plane (b), and fold amplitude ratio (c) with increasing shortening for the individual sequential folds (individual anti- and synforms; thin lines) and the bulk fold structure (thick lines) for the same simulation as in Figure 2. The bulk fold amplitudes in z- and y-direction are equal to the individual fold amplitudes of the initial fold. All values are normalized by the initial amplitude in each corresponding direction. b) and c) are derived from a). Vertical gray lines indicate the first appearance of sequential folds.
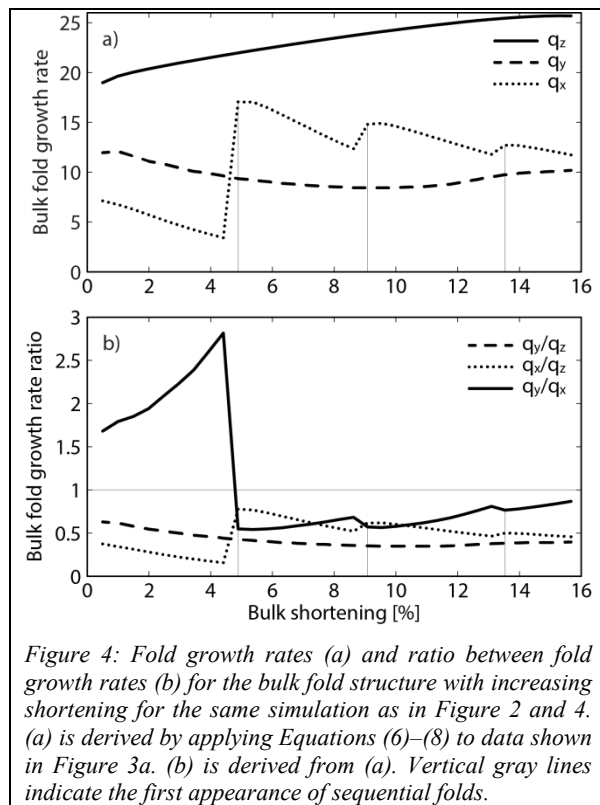
Figure 4: Fold growth rates (a) and ratio between fold growth rates (b) for the bulk fold structure with increasing shortening for the same simulation as in Figure 2 and 4. (a) is derived by applying Equations (6)–(8) to data shown in Figure 3a. (b) is derived from (a). Vertical gray lines indicate the first appearance of sequential folds.

4. Discussion

Recently, interest in the lateral growth and linkage process of natural folds has been renewed by the oil- and gas-industry because it can lead to compartmentalization of structurally controlled reservoirs within an anticline. Previous studies only considered fold elongation to explain the linkage process (Bretis et al., 2011; Grasemann and Schmalholz, 2012), without including the second lateral growth direction (sequential fold growth). However, this study demonstrates that both lateral growth directions are equally important. In case two initially isolated fold structures grow in all three directions, the initial fold of one structure (0th sequential fold) may well link with the 1st sequential fold of the second structure. Grasemann and Schmalholz (2012) termed this scenario *no linkage*, yet it is equally important for understanding linked bulk fold structures and the term *1st order linkage* is proposed here. Accordingly, Grasemann and Schmalholz (2012)'s *linear linkage* and *oblique linkage* scenarios (linkage of two initial folds) are categorized as *0th order linkage*.

The numerical simulations represent simplified test cases in that they only comprise a two-layer system, linear viscous (Newtonian) rheology, and no erosion at the upper surface. Therefore, the modeled geometries may not be translated one-to-one to natural fold structures. However, the aim of these simulations is to demonstrate first-order phenomena of 3D fold growth. The general result of almost equal fold growth rates in both lateral directions (fold elongation and sequential fold growth) and slightly larger fold growth rate in vertical direction (fold amplification) is expected to still hold in more realistic modeling scenarios or natural situations.

5. Conclusions

Numerical 3D folding simulations using a range of parameter combinations demonstrated that a fold structure grows in the two lateral directions with similar rates while the fold amplification rate is slightly higher. Such growth behavior results in fold structures that hardly change their bulk aspect ratio with increasing shortening. If a fold structure originates from an isolated perturbation (e.g., diapir) its aspect ratio remains roughly 1:1; if a fold structure originates from a line perturbation (e.g., fault) its aspect ratio remains large. However, large-aspect ratio fold structures can also be formed by linkage of two or more individual fold structures. Thereby, higher-order linkage (linkage between sequential folds of different order) is equally important as 0th order linkage because of the equal fold growth rates in the two lateral directions.

References
Bretis, B., Bartl, N. and Grasemann, B., 2011. Lateral fold growth and linkage in the Zagros fold and thrust belt (Kurdistan, NE Iraq). Basin Research, 23, 615–630.

Fletcher, R.C., 1991. Three-dimensional folding of an embedded viscous layer in pure shear. Journal of Structural Geology, 13, 87–96.

Frehner, M., 2011. The neutral lines in buckle folds. Journal of Structural Geology, 33, 1501–1508.

Frehner, M. and Schmalholz, S.M., 2006. Numerical simulations of parasitic folding in multilayers. Journal of Structural Geology, 28, 1647–1657.

Grasemann, B. and Schmalholz, S.M., 2012. Lateral fold growth and fold linkage. Geology, 40, 1039–1042.

Hudleston, P.J. and Treagus, S.H., 2010. Information from folds: A review. Journal of Structural Geology, 32, 2042–2071.

Schmid, D.W., Dabrowski, M. and Krotkiewski, M., 2008. Evolution of large amplitude 3D fold patterns: A FEM study. Physics of the Earth and Planetary Interiors, 171, 400–408.